Influence of Various Reaction Media on the Thermal and Rheological Properties of Poly(acrylamide-co-N-hexadecylacrylamide)

Shadi Hassanajili,[1] Elaheh Abdollahi[2]

[1]Chemical and Petroleum Engineering School, Shiraz University, 71348-51154 Shiraz, Iran
[2]Department of Chemical Engineering, Islamic Azad University of Fars Science and Research Branch, Iran
Correspondence to: S. Hassanajili (E-mail: ajili@shirazu.ac.ir)

ABSTRACT: A hydrophobically modified polyacrylamide (PAM) was synthesized by the copolymerization of acrylamide (Am) and N-hexadecylacrylamide (hAm) through solution copolymerization in a polar organic solvent. Polymer synthesis was performed in three nonaqueous media, including dimethyl sulfoxide (DMSO), a mixture of DMSO and an anionic surfactant such as sodium dodecyl sulfate, and a mixture of DMSO and an acidic surfactant such as dodecyl benzene sulfonic acid. The obtained copolymer, poly(acrylamide-co-N-hexadecylacrylamide) [poly(Am-co-hAm)], was characterized by ^{1}H-NMR. The physical properties of poly(Am-co-hAm)s synthesized in different media were compared with those of PAM and with each other by viscosity measurement, X-ray diffraction, thermogravimetric analysis, and differential scanning calorimetry. We investigated the ways in which the polymerization medium affected the hydrophobic distribution within the resulting copolymer structure. This aspect, in turn, should have altered the solution properties and the microstructure of the copolymer. For this purpose, we studied the viscometric behavior in diluted solutions, the thermal behavior and thermal stability of the copolymers, and finally, the crystalline structure of the copolymers. © 2013 Wiley Periodicals, Inc. J. Appl. Polym. Sci. 2014, 131, 39939.

INTRODUCTION

One of the most significant advances made in water-soluble polymers in the last 3 decades has been their modification with hydrophobic moieties.[1] Hydrophobically modified or water-soluble associative polymers are now routinely used in technical formulations to modify the rheological properties of solutions or increase the stability of dispersions.[2,3] The incorporation of a few hydrophobic groups in a hydrophilic macromolecule chain-like polyacrylamide (PAM) results in a system with unique rheological characteristics. In an aqueous solution, the hydrophobic groups tend to associate, and their direct contact with water is restricted; this leads to substantial rheological effects.[4] The association of hydrophobic moieties in nanodomains in hydrophobically modified polymers[3] gives rise to unusual properties in water and rheological properties for different applications because there are strong intramolecular and intermolecular associations between the hydrophobic units.[5,6] Thereby, aqueous solutions of hydrophobically associating polymers exhibit very interesting rheological properties and higher thickening capabilities compared to unmodified precursors.[7] PAM as a water-soluble backbone in hydrophobically associating polymers find applications in a wide variety of areas, which include polymer drug delivery to systems,[8] coating industry[9] rheology modifiers in various processes as thickeners,[10] or modifier in the formulations of enhanced oil recovery.[11–15] However, PAM can present some limitations when it is subjected to elevated shear rates; this leads to losses in the viscosity. To prevent such difficulties, a surface-active monomer, or surfmer, which is one type of polymerizable functional surfactant with hydrophilic and hydrophobic moieties, can be used as a hydrophobic monomer to copolymerize with Am to obtain hydrophobically associative polyacrylamide (HAPAM).[16]

Hydrophobically modified water-soluble polymers such as HAPAM can be synthesized by two routes: (1) copolymerization of a hydrophilic monomer with a hydrophobic monomer, which requires a surfactant for its solubilization, and (2) posthydrophobic modification of a polymer.[13,15,17–22] The former reaction route proceeds in one step. However, the insolubility of the hydrophobic monomer in water can generate some difficulties.[21]

The latter reaction route consists of two steps; first, the polymer is dissolved in a solvent, and then, polymer functional groups react with the reactant modifying agent. Unlike nonpolymeric materials, the polymers do not dissolve instantaneously, and the

dissolution is controlled by either the disentanglement of the polymer chains or the diffusion of the chains through a boundary layer adjacent to the polymer–solvent interface.[22] The post-modification of PAM is performed by the direct N-alkylation of the parent PAM at a very low concentration and a high consumption of dimethyl sulfoxide (DMSO) in homogeneous conditions at a high temperature and long duration because of the poor solubility of PAM in DMSO.[21,23]

On the basis of other workers' reports, in the homogeneous copolymerization, the hydrophobic groups are randomly distributed along the copolymer backbone, but the micellar copolymerization in water favors a blocky distribution because of the high local concentration of hydrophobic monomers in the micelles.[17] Therefore, the heterogeneity in a copolymerization system can be improved with a suitable solvent such as DMSO for both water-soluble and water-insoluble monomers. In this way, a microhomogenized media may be obtained with better matching between the feed and product compositions. DMSO is a unique solvent with very low toxicity to humans and the environment. It is a recyclable and environmentally compatible solvent that is present in many food products and plays a significant role in nature's global sulfur cycle. DMSO is a highly polar, aprotic solvent that dissolves a wide array of organic molecules, both polar and nonpolar.[24–28]

In this study, we designed three reaction media for the synthesis of water-soluble associative copolyacrylamide based on hydrophobically modified acrylamide (Am). Here, DMSO and mixture of DMSO with surfactants were used as reaction media, and Am was copolymerized with N-hexadecylacrylamide (hAm) through radical polymerization. hAm is an Am with a long hydrocarbon tail, which makes it water-insoluble even in the presence of a surfactant after 24 h of mixing at 60°C (this was experimentally confirmed). In this study, we performed copolymerization in DMSO, the suitable organic solvent that not only dissolved Am but also perfectly dissolved hAm in a very short time (10 min) at a mild temperature (60°C). The aim of this study was to design an appropriate one-component solvent as reaction medium for simultaneously dissolving hydrophobic and hydrophilic monomers to attain a more efficient introduction of a higher percentage of hydrophobic monomer (5% mol) in the hydrophilic backbone of PAM with controllable distribution. In the first part of this study, we characterized the hAm comonomer and Am–hAm copolymer by NMR spectroscopy. Then, the effects of the reaction media on the microstructural
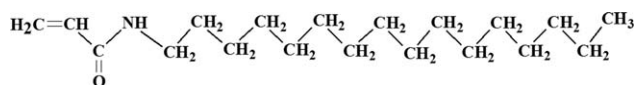

Figure 1. Chemical structure of hAm.

formation of the copolymers and their physical properties were investigated with thermogravimetric analysis (TGA), differential scanning calorimetry (DSC), and rheological tests.

EXPERIMENTAL

Materials
Am (Merck), DMSO (99.5%, Aldrich), potassium persulfate (KPS; $K_2S_2O_8$), dried acetone (C_3H_6O), and chloroform ($CHCl_3$) were all received from Merck and were used as received. Other chemicals, including sodium dodecyl sulfate (SDS) and dodecyl benzene sulfonic acid (DBSA), were also purchased from Merck.

Synthesis of the hAm Comonomer and Am–hAm Copolymer
hAm was prepared according to a reported procedure from the N-alkylation of acrylamide[29] and characterized by melting temperature (T_m) analysis, Fourier transform infrared (FTIR) spectroscopy, and ^{1}H-NMR spectroscopy. The characterization data were in agreement with the proposed structure of the products. The T_m of hAm was 63°C. The hAm structure is shown in Figure 1.

P(Am–hAm)s were prepared by the radical solution copolymerization of Am and a small amount of hAm as a hydrophobic monomer in DMSO with KPS as the initiator (Scheme 1). Table I shows the reaction conditions of polymer synthesis. The synthesis procedure of P_1 is described here: first, a mixture of 0.32 g of hAm (10.84×10^{-4} mol), 1.5 g of Am (2.11×10^{-2} mol) was grind-milled completely for 2 min and placed in a 25-mL round-bottom flask. Then, 4.0 mL of DMSO was added. The mixture was heated in an oil bath gradually from room temperature (RT) up to 65–70°C, for 10 min. Then, 0.5 mL of a 0.058 g/mL KPS solution in DMSO was added to the mixture. After 10 min, its temperature was reduced to 55–60°C, and polymerization proceeded for a period of 110 min. The resulting product was isolated by the addition of 10 mL of acetone. The white solid was filtered off and added to 4 mL of chloroform drop by drop to eliminate any unreacted monomers inside the polymers. The polymer was dried in vacuo at 45°C for 5 h to give 1.72 g (94.5%) of P_1. Polymers P_2 and P_3 were each synthesized in a mixture of DMSO and their corresponding surfactants (Table
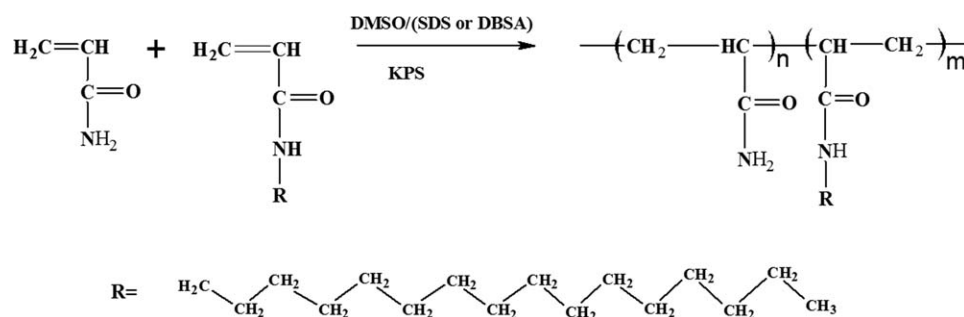
Scheme 1. Copolymerization reaction of Am with hAm.

Table I. Reaction Conditions of Polymerization[a]

Polymer	I% (g/g)[b]	M% (g/g)[c]	[hAm]/[S] (mol/mol)	Solvent	Surfactant
P_1	0.47	28.66	0.0	DMSO	-
P_2	0.47	28.66	0.52	DMSO	SDS
P_3	0.47	28.66	0.52	DMSO	DBSA
PAM	0.47	28.66	0.0	DMSO	-

[a] M = monomer, I = initiator, S = surfactant. The time of the reaction was 110 min at 55–60°C.
[b] I% = [Mass of initiator/[mass of (initiator + monomer + solvent)]] × 100.
[c] M% = [Mass of monomer/[mass of (initiator + monomer + solvent)]] × 100.

II), SDS and DBSA, respectively. Each surfactant was added to DMSO at molar ratio of surfactant to hAm of 0.52. The concentration of surfactants was higher than the critical micelle concentration of SDS in pure DMSO; this was determined in agreement with the results reported by Johans and Suomalainen.[30] Surfactants can form micelles in a strongly polar solvent such as formamide with qualitatively the same features as in water[31] but at a much higher critical micelle concentration. The copolymers were hydrolyzed in a 1M NaOH solution at 80°C for 5 h. PAM was synthesized in DMSO as a reference polymer under identical conditions.

Characterization

^{1}H-NMR (250-MHz) spectra were recorded on a Bruker Avance 250 instrument in hexadeuterated dimethyl sulfoxide (DMSO-d_6) at RT. FTIR spectra were recorded on a Jasco FTIR spectrophotometer. The IR spectra of the solids were obtained with KBr pellets. Vibrational transition frequencies are reported in wave number (cm^{-1}). The band intensities and designations are assigned as weak (w), medium (m), shoulder (sh), strong (s) broad (br), stretching (st), and bending (bend). The inherent viscosities were measured by a standard procedure with a Cannon–Fensk Routine Viscometer and a rotational viscometer on a Dv2 viscometer v6.3. The TGA data for the polymers were recorded by a Mettler-Toledo TG-50 thermal analyzer under an N_2 atmosphere at a heating rate of 20°C/min. The DSC data for the polymers were recorded on a DSC-30/S instrument under an N_2 atmosphere. The glass-transition temperatures (T_gs) were recorded at the onset of the transition in the heat capacity taken from the heating DSC traces. The sample was first scanned from RT to 140°C and maintained for 1 min; this was followed by quenching to −80°C at a cooling rate of 20°C/min, and then, a second heating scan was used to measure the sample's T_g of the hydrophobic segment or the T_m of the crystalline segment at a heating rate of 20°C/min. Wide-angle X-ray diffrac-

tion (WAXD) measurements were carried out with a Philips Analytical X'Pert diffractometer with graphite monochromatized Cu Kα radiation (40 kV; 30 mA) in a continuous scanning mode.

The intrinsic viscosities of the polymers were determined in a DMSO and water solution at 22°C. Measurements were carried out with an automatic capillary viscometer (Ubbelohde type) at polymer concentrations ranging from 0.01 to 0.05 g/dL. The shear rate imposed on the capillary did not affect the viscosity data with the values obtained (<65 mL/g). In these experiments, care was taken to prevent foaming of the copolymer solutions, which would result in erroneous flow times.

The rheometric analysis of dilute polymer solutions was carried out at RT in the concentration range 0.04–0.065 g/mL. Polymer solutions were prepared by the dissolution of the samples in DMSO and water at appropriate concentrations with magnetic mixing at RT. Before the measurements, the solutions were kept still for 3 more days to eliminate air bubbles. The instrument was interfaced with a personal computer and driven by a software package (Carri45) supplied by the manufacturer. The shear rate ranged from 0.3 to 130 rpm.
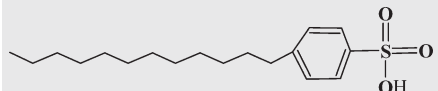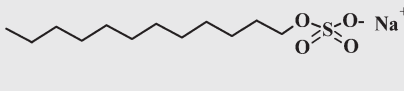
RESULTS AND DISCUSSION

hAm Comonomer (hAm) Characterization

hAm (hAm) was synthesized via an alkylation reaction of Am according to previous work by Lele et al.[29] The chemical structure and purity of hAm were confirmed by T_m measurement, FTIR spectroscopy, and ^{1}H-NMR spectroscopy. The reduction of the T_m from 80°C for Am to 65°C for hAm was due to substituted NH_2 by N-hexadecyl, which reduced the Am hydrogen bonding and its crystallinity. The FTIR spectra of hAm in Figure 2 shows peaks that confirmed that its chemical structure contained absorption bands of terminal methyl (CH_3), methylene (CH_2), NH(II), and carbonyl amide (—NH—C=O) groups and a peak at 3300 cm^{-1} (m, stretching) for amide groups linked to alkyl groups [NH(II)], which confirmed the reaction of amide in Am with alkyl groups and the transfer from a primary amide nitrogen (NH_2) to a secondary amide nitrogen (NH—CH_2—). There were peaks at 1600–1651.73 cm^{-1} (s, stretching and bending) for C=C, C=O, and N—H groups; 1549.22 cm^{-1} (m, stretching) for C—N groups; 720 cm^{-1} (s, bending) for the bending motion of long alkyl chain groups; 1470 cm^{-1} (s, bending) for CH_2; and 1375 cm^{-1} (s, bending) for CH_3.

As shown in Figure 3, the ^{1}H-NMR spectrum of hAm revealed the presence of peaks at 0.5–1.5 ppm, which indicated the substitution of the hydrogen of NH_2 in Am by N-hexadecyl chains; protons in the terminal methyl group indicated at 0.9 ppm (d,

Table II. Chemical Structure of the Surfactants

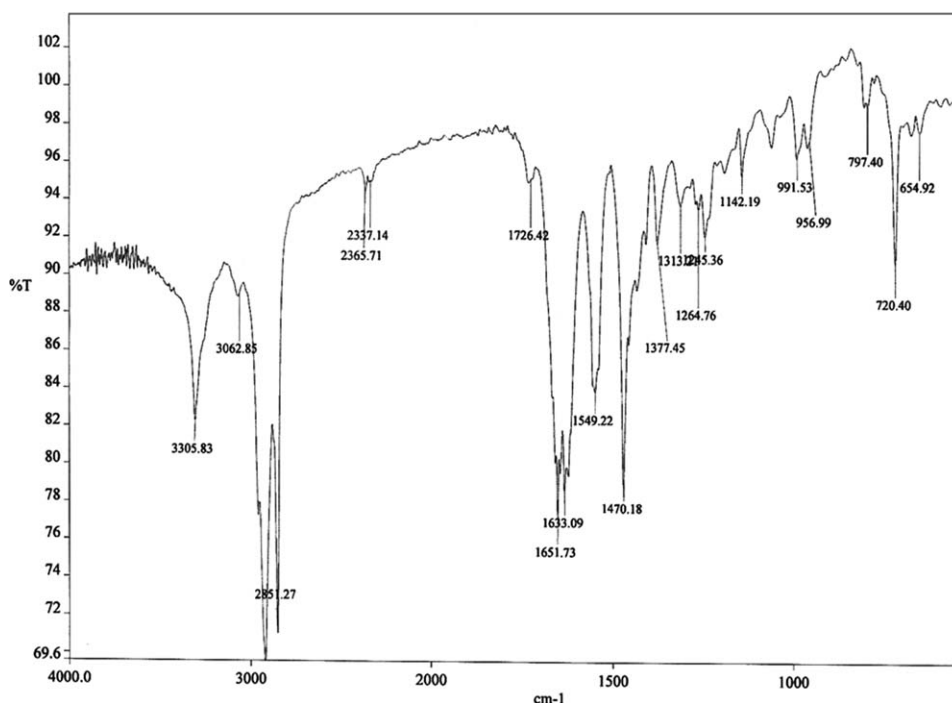| DBSA	SDS

Figure 2. FTIR characterization of the hAm comonomer.

3H, CH$_3$); protons in methylene linked to the NH amide group at 3.2 ppm (c, weak, 2H); protons in methylene in the alkyl chain group at 1.3 ppm (d, 28H); and protons of alkene CH$_2$=CH at 4.5–6.5 ppm, which confirmed the alkene groups in Am that were left unreacted.

Am–hAm Copolymer Characterization

To confirm chemical structure of the copolymer, we selected ^{1}H-NMR spectroscopy because in ^{1}H-NMR the eliminated hydrogen of sp^2 was confirmed by the disappearance of peaks at 4.5–6.5 ppm according to the standard ^{1}H-NMR peak of Am. In Figure 4, the ^{1}H-NMR spectrum of P$_1$ shows the existence of peaks at 0.8–1.5 ppm, which indicate the inclusion of hexadecyl chains in the polymer structure, protons in the terminal methyl

group at 0.9 ppm (E, 3H, CH$_3$), protons in methylene linked to NH amide groups at 3.2 ppm (C, weak, 2H), protons in methylene in the alkyl chain groups at 1.3 ppm (D, 28H), and the aliphatic region from the PAM backbone present at 1.5–2.5 ppm (A, B, CH$_2$).

Hydrophobic Content. ^{1}H-NMR spectroscopy is a method commonly used for the determination of copolymer microstructures in place of traditional methods such as elemental analysis because of the very low percentage of hydrophobic monomer in the polymer. It is, however, generally less accurate than UV spectroscopy for determining the hydrophobic content, although it is still convenient when the hydrophobic content is
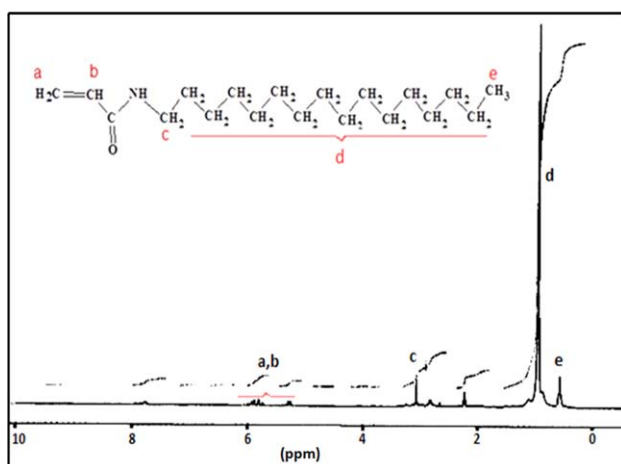

Figure 3. ^{1}H-NMR (250-MHz) spectrum of the comonomer (hAm) in DMSO-d_6 at RT. [Color figure can be viewed in the online issue, which is available at wileyonlinelibrary.com.]
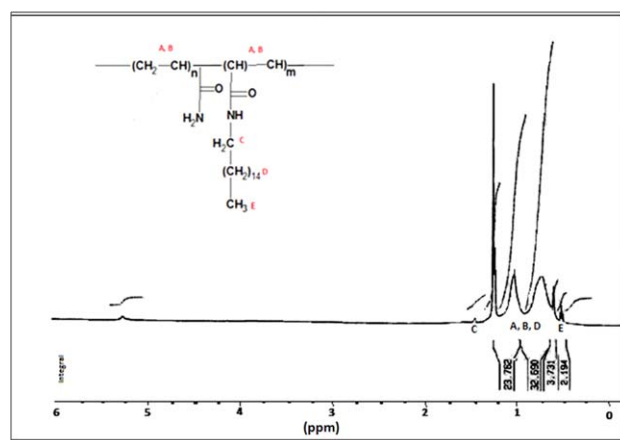

Figure 4. ^{1}H-NMR (250-MHz) spectrum of the copolymer P$_1$ in DMSO-d_6 at RT. [Color figure can be viewed in the online issue, which is available at wileyonlinelibrary.com.]
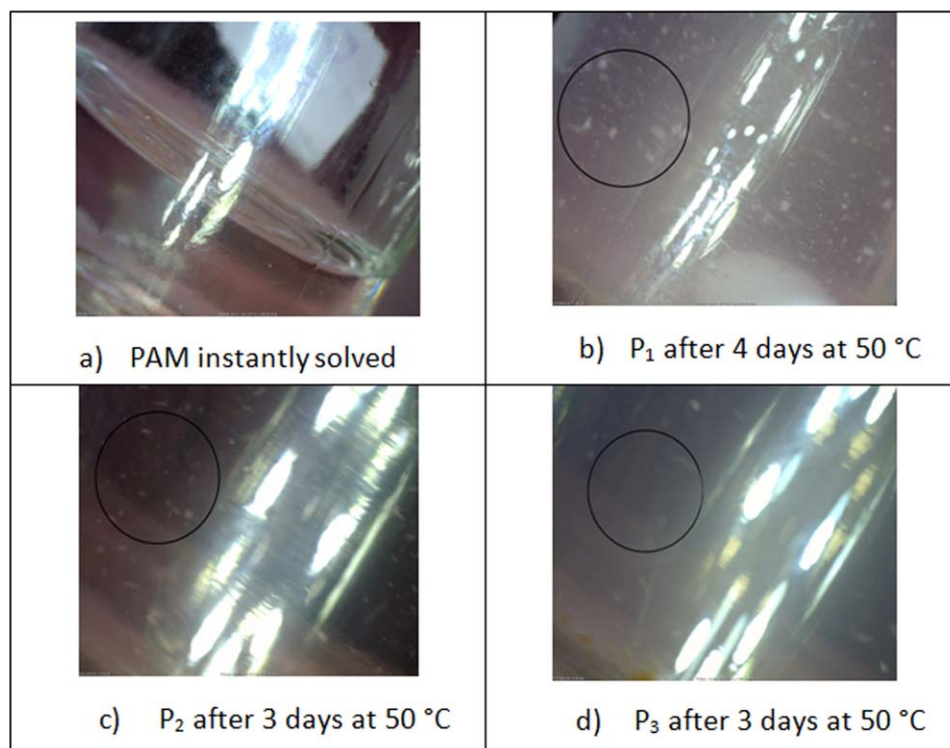
Figure 5. Macro images of the water polymer solutions (2000 ppm): (1) PAM optically transparent solution, (2) insoluble P_1 giving an opaque solution, (3) poorly soluble P_2 with relative clarity, and (4) sparingly soluble P_3 giving an opaque solution (captured by a Dinocapture camera). [Color figure can be viewed in the online issue, which is available at wileyonlinelibrary.com.]

sufficiently high (>2 mol %) or when the hydrophobic moiety contains two terminal methyl groups, as in case of *N,N*-dihexylacrylamide. Consequently, in most studies, the hydrophobic content is assumed to be equal to the initial feed composition.[23,32] According to the expected chemical structure of the prepared copolymers, their NMR spectrum was different from that of PAM in protons of methylene groups and protons in the terminal methyl group of the alkyl chain of hAm. By calculating the number of different protons in the copolymer, we determined the hydrophobic content from the integrated area (S) of the protons in CH_3 and CH_2 in the alkyl chain and CH in the main polymer backbone. The hydrophobic content was calculated with eq. (1):

$$S(E)/[S(A)+S(B)+S(D)] \qquad (1)$$

where $S(E)$ is the integrated area of the protons in CH_3, $S(A)$ and $S(B)$ are the integrated areas of the protons from the CH groups in the polymer backbone, and $S(D)$ is the integrated area of the protons in CH_2 in the alkyl chain of hAm (Figure 4). The hydrophobic content for the copolymers, which was calculated according to eq. (1), amounted to 5% mol for P_1.

Effect of hAm Inclusion on the Polymer Chain Solubility in Water

First, to examine the effect of the hydrophobic monomer that was introduced into the polymer backbone, we prepared a mixture of polymers in water. PAM formed an optically transparent solution instantly, whereas the copolymers were visibly suspended in water, even after mixing and heating for some days, which did not help to make a perfect solution in water. Figure 5 shows a macroscale depiction of the polymer solution. As predicted, P_1 displayed a different microstructure because it was less soluble than P_2 and P_3. Then, the copolymers were hydrolyzed in water to be solubilized in water. As a result, the inclusion of a small amount of hydrophobic monomer (5% mol) in the PAM backbone made it insoluble in water.

Viscosity

According to Figure 6, P_1, P_2, and P_3 had higher viscosities than PAM. The presence of hydrophobic groups in the
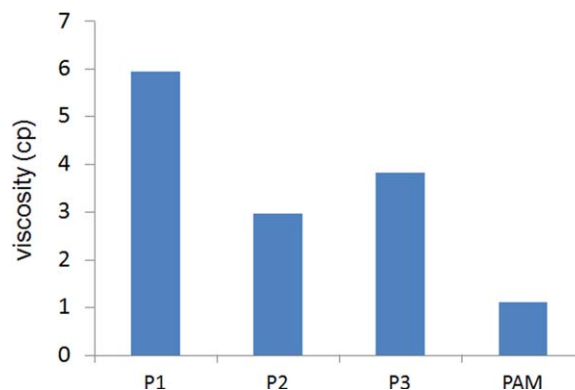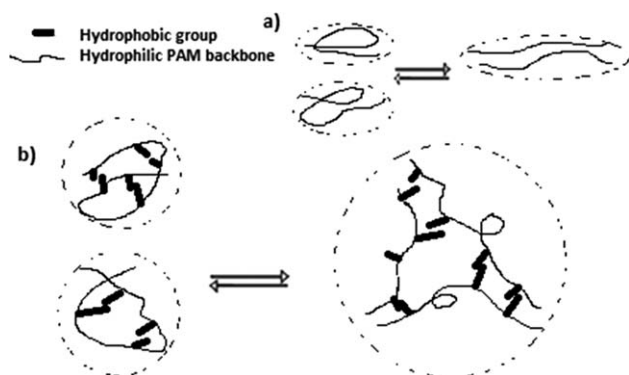

Figure 6. Viscosity values of the copolymers and a reference polymer, PAM (concentration = 8000 ppm in DMSO at RT). [Color figure can be viewed in the online issue, which is available at wileyonlinelibrary.com.]

Scheme 2. Intramolecular and intermolecular interactions effects on the hydrodynamic volume of (a) PAM and (b) poly(Am-*co*-hAm).

Table III. E_a (J/mol) Values of the Copolymers and PAM

Polymer	P_1	P_3	PAM
E_a (J/mol)	28,342	11,099	8505

backbone of the copolymer made it more viscous because of an excluded volume effect. Very long hydrophobic groups of hAm in the copolymers interacted with each other upon intermolecular and intramolecular interactions in the crystalline matrix of the PAM backbone. These led to an increase in the hydrodynamic volume, which in turn, yielded a polymer with a much better thickening capability[23] compared to their nonassociative analogue (PAM; Scheme 2).

Viscosity–Temperature Relationship. Figure 7 shows the intrinsic viscosity–temperature relationship for the copolymers and PAM. The increase in temperature caused a total sharp drop in the viscosity of the polymers. All of the copolymers showed different behaviors compared to PAM. They showed significant thermothinning with increases in temperature and a sudden, small thickening at 60°C. This behavior was related to the complex development in elongation and the conformation of alkyl groups in the hAm monomer. This was because of weaker interaction sites between the hydrophobic chains compared to amidic interactions in PAM.

One of the major parameters of a polymer solution is the activation energy of viscous flow (E_a). It can serve as a criterion of

strength of intermolecular interactions. This parameter is determined from the temperature dependence of the viscosity (η; Figure 7) in Arrhenius coordinates. This can be described with the Arrhenius–Frenkel–Airing equation:

$$\eta = B \exp (Ea/RT) \qquad (2)$$

where B is the empirical parameter, T is temperature (K) and R is the universal gas constant. The value of E_a is calculated by evaluation of the slope ratio of $\ln([\eta])/(1/T)$. The HAPAM solution was characterized by a higher E_a. As shown in Table III, the copolymers displayed a higher activity because of their higher viscosity compared to that of PAM.

Rheological Study in Dilute Solution

The thickening properties of hydrophobically modified PAMs were strongly dependent on the experimental conditions of the synthetic procedure.[17] Figure 8 shows the viscosity versus the shear rate for copolymer solutions in DMSO as a polar solvent at RT in three shear rate zones: low, moderate, and high. Generally, at a shear rate below 5 s^{-1}, the viscosity increases with increasing shear rate because of the augmentation of the intermolecular hydrophobic interaction; this is generally attributed to a change from intramolecular to intermolecular interactions.[33] A nonhomogeneous distribution of the hydrophobes within the hydrophobic clusters and their redistribution upon the application of stress can be one of the reasons for this behavior.[34] At a moderate shear rate, the intermolecular associations dissipate and lead to shear-thinning behavior, and finally, at a high shear rate, there is a slight thinning behavior displayed because of the balance between the intermolecular association and disassociation. This behavior exhibits the pseudoplastic nature of these copolyacrylamides in DMSO. This behavior shows that intermolecular association is a reversible process, and therefore, all intermolecular aggregations are disrupted at a high shear rate. As shown in Figure 8(a), at low shear rates, the shear-thickening behavior was also attributed to the expansion of polymer chains and the transition of intramolecular associations to intermolecular associations. In case of P_3, this thickening happened at higher shear rates compared to those of P_1 and P_2. As shown in Figure 8(b), with increasing shear rate to a value of 15 s^{-1} (thinning zone), the rate of the reduction in viscosity was different for copolymers synthesized in different media. Compared to that in P_3, the shearing in P_1 and P_2 lowered the viscosity more sharply. This result demonstrated the more blocky distribution of hydrophobic chains in P_1 and P_2. With increasing shear rate, the blocky hydrophobic associations were suddenly destroyed, and a sharp thinning occurred, but in case of P_3, hydrophobic associations were distributed homogeneously along the crystalline backbone, and they were gradually destroyed. As shown in Figure 8(c), with a very high shear rate (>15 s^{-1}), the viscosity decreased much more slowly, and a rather shear, rate-independent viscosity (Newtonian plateau)
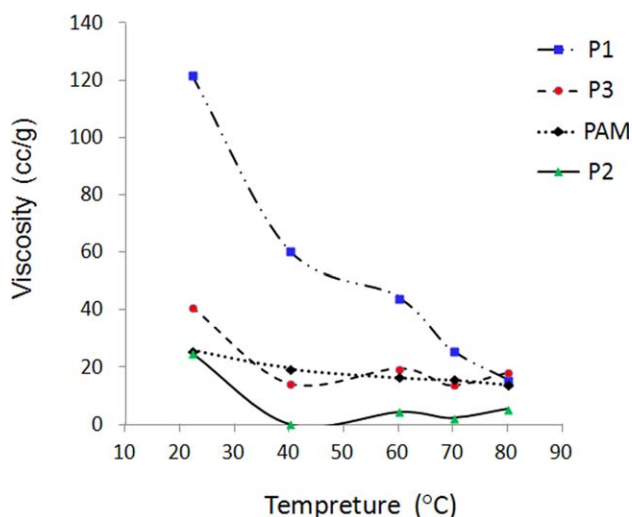

Figure 7. Viscosity versus temperature for the copolymers and PAM solutions in DMSO. [Color figure can be viewed in the online issue, which is available at wileyonlinelibrary.com.]
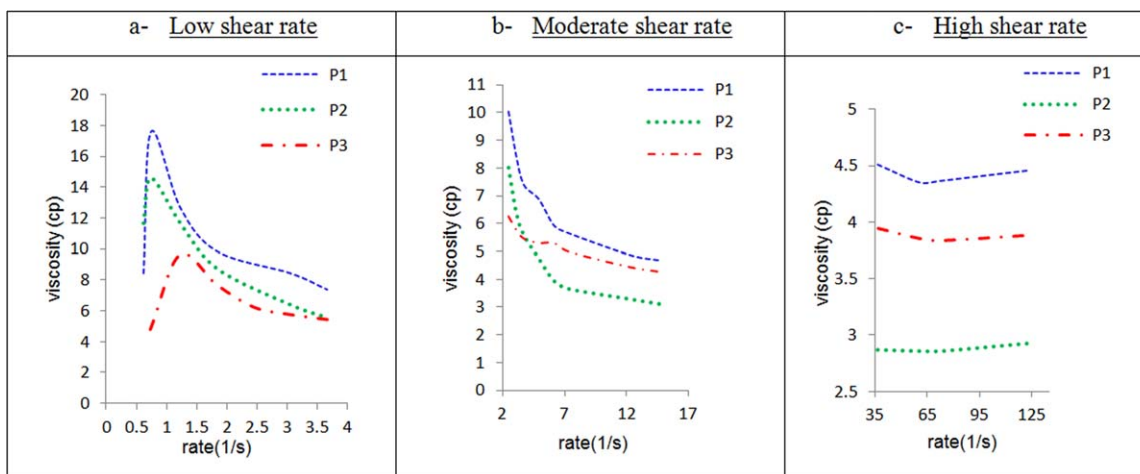
Figure 8. Viscosity versus the shear rate for the 3500 ppm polymer solution in DMSO at RT. [Color figure can be viewed in the online issue, which is available at wileyonlinelibrary.com.]

was observed at high shear rates. This observation was similar to that frequently observed for hydrophobically modified associative polymers.[33] When the shear rate was above 70 s^{-1}, a shear-thickening effect was obtained for P_2 and P_3, whereas for P_1, this thickening effect occurred at shear rate of 60 s^{-1}.

Figures 9 and 10 show the viscosity versus the shear rate for the polymer solutions in H_2O at RT. The total behavior in H_2O was the same for DMSO, where thickening appeared at lower shear rates followed by a shear thinning, and there was thickening behavior at a high shear rate for all of the polymers. At a very low shear rate (0.5–1 s^{-1}), PAM, P_2, and P_3 displayed shear thinning (a viscosity drop), and with increasing shear rate at 1–4 s^{-1}, PAM showed Newtonian behavior followed by a shear-thinning effect, but copolymers P_2 and P_3 showed a

shear-thickening effect followed by shear thinning. This thickening behavior showed a transition from intrachain alkyl groups to interchain entanglement, but PAM did not present such an effect because of the absence of hydrophobic groups. For P_3, this thickening started sooner and in a wider shear range (1.224–2.448 s^{-1}), but for P_2, it started later with a shorter shear range (1.88–2.488 s^{-1}). In the case of P_3, high-density hydrophobic intramolecular entanglements were broken by shearing, intermolecular hydrophobic entanglements started to arrange, and the viscosity increased even further. With P_2, the viscosity decreased slightly with shearing (at <2 s^{-1}) and then started to thicken under higher shear rates (1.8–2.4 s^{-1}). At a high shear rate (>30 s^{-1}), the polymers showed a critical shear rate at a point where the shear thinning changed into shear thickening. This behavior was the same as the rheological behavior of the hydrolyzed PAM backbone in a water solution at high shear rates. Although the hydrolyzed PAM solutions displayed pseudoplastic behavior (shear thinning) in simple viscometers, it has been demonstrated that these solutions show dilatant characteristics (shear thickening) in porous media and in viscometers at relatively high shear rates. Research has demonstrated the presence of a critical shear rate at which the shear-thickening behavior arises in viscometers.[35] This critical shear rate occurred at higher values for P_2 and P_3 than for PAM (Figure 10).

Effect of the Solvent on the Rheological Behavior. Figure 11 shows the different rheological behaviors at low shear rates for P_2 and P_3 in two polar solvents, water with perfect polarity and DMSO with hydrophobic parts (methyl) and a hydrophilic sulfoxide moiety (Figure 12). The copolymer could interact hydrophobically with the methyl groups in DMSO by hydrophobic alkyl chains. As shown in Figure 11, at low shear rates (0.5–1.5 s^{-1}) in DMSO solution of copolymers, the methyl–alkyl chain interactions became stronger so shear thickening appeared in this early stage; this was followed by shear thinning at higher shear rates (>1.5 s^{-1}). In contrast, in water solution, shear thinning was followed by a thickening effect. This behavior in water is commonly found for many hydrophobic systems,[36–38]
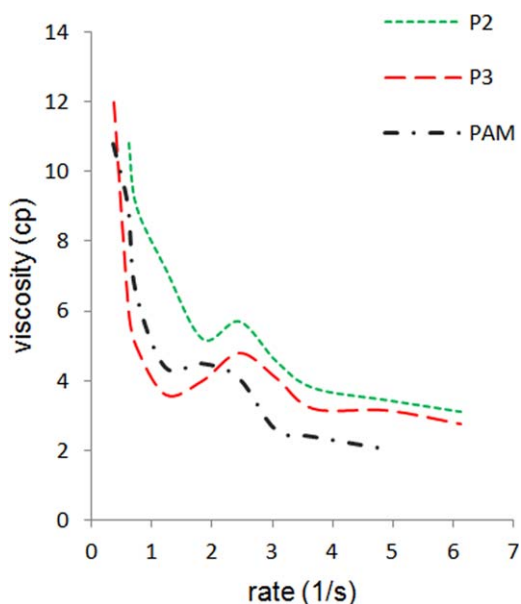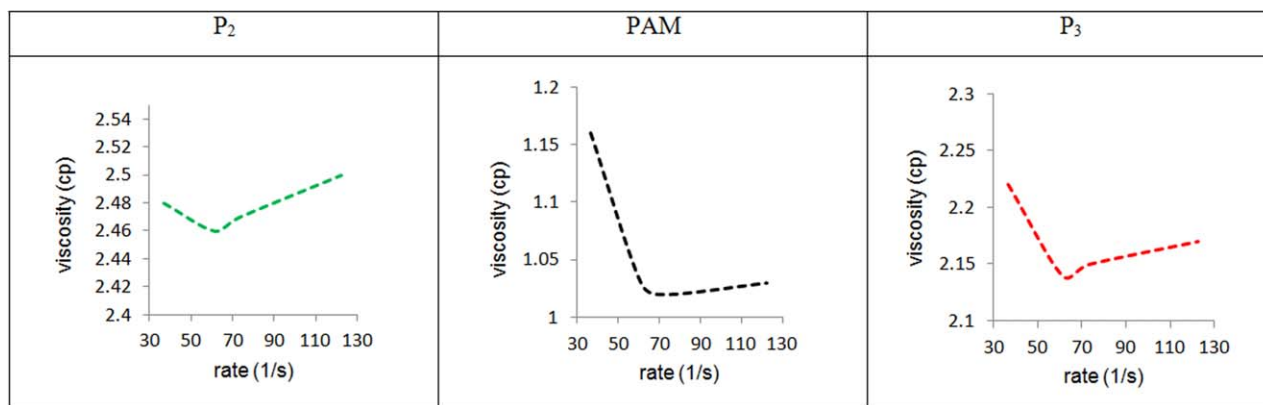

Figure 9. Viscosity versus the shear rate for the water polymer solutions (5000 ppm) at RT (low shear rate). [Color figure can be viewed in the online issue, which is available at wileyonlinelibrary.com.]

Figure 10. Viscosity versus the shear rate for the polymer solution (5000 ppm) in H_2O at RT (high shear rate). [Color figure can be viewed in the online issue, which is available at wileyonlinelibrary.com.]
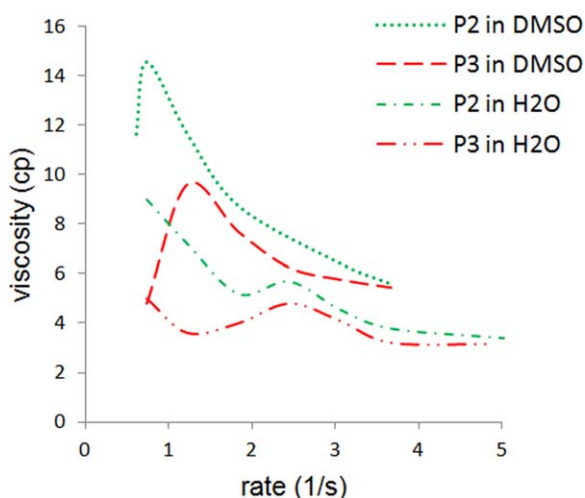

Figure 11. Rheological behavior of the copolymer solutions in H_2O and DMSO at RT. [Color figure can be viewed in the online issue, which is available at wileyonlinelibrary.com.]

and it is generally attributed to a change from intramolecular to intermolecular interactions in copolymer molecules.

Comparing the P_2 and P_3 behaviors in two solvents, we found that in DMSO, P_3 started thickening later but still held thickening at a wider range of shear rates (0.5–1.5 s^{-1}). In water, P_3 started thickening sooner but started thinning simultaneously with P_2 at 2.448 s^{-1}. It seemed that there was a different distribution of hydrophobic monomer in the polymer backbone, and so different rheological behaviors were observed.

Figure 12. Chemical structure of DMSO. [Color figure can be viewed in the online issue, which is available at wileyonlinelibrary.com.]

Thermal Analysis

Effect of the Temperature on the Viscosity. As shown in Figure 7, although the polymers showed thermothinning, the copolymers showed this property much more strongly. A reduction in the solution viscosity with increasing temperature has been reported for solutions of hydrophobically associating water-soluble polymers.[4,39–42] The hydrophobic effect was weakened at elevated temperatures because of the increased mobility of the copolymer chains, so a sharper decrease in the copolymer viscosity occurred; this gave rise to a loss of hydrophobic inter-chain entanglements and/or an increase in the copolymer solubility with linear conformation. This hydrophobic interaction did not exist in PAM, so the viscosity reduction was not significant. As shown in Figure 7, this thermothinning was more unnoticeable in P_2 and P_3 compared to P_1 because of their different microstructures.

According to Figure 13, the thermoviscosity behaviors in water and DMSO showed that the viscosity drop for the copolymers
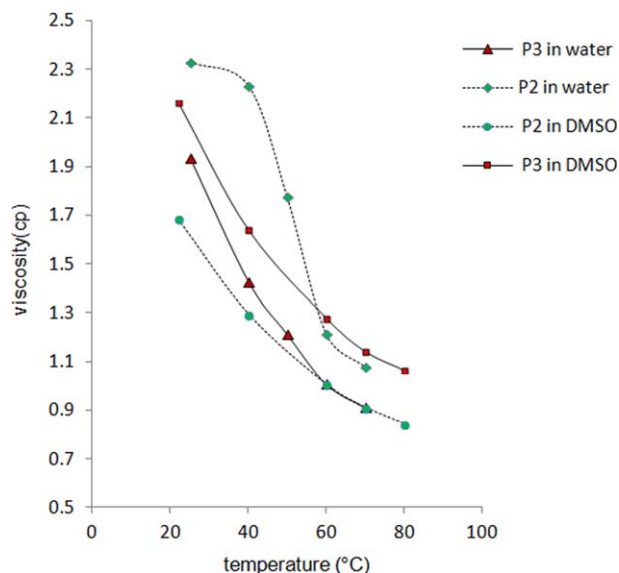

Figure 13. Viscosity versus the temperature for the copolymers and PAM solutions in H_2O. [Color figure can be viewed in the online issue, which is available at wileyonlinelibrary.com.]

was sharper in water than in DMSO. The viscosity of P_2 in water was almost unchanged but decreased markedly up to 40°C, and in contrast, the viscosity of P_2 in DMSO decreased considerably with temperature. The viscosity of P_3 in both water and DMSO decreased sharply with temperature.

Thermal Stability of the Polymers. The thermal stability of the copolymers was investigated by thermogravimetric analysis. Figure 14 shows the TGA and differential thermogravimetric analysis (DTGA) results of PAM and its copolymers. From the DTGA curves, we noted that all of the polymers had two important mass loss stages. We identified two distinct stages of the thermal decomposition of the polymer backbone. Stage 1, in the temperature range of 190–350°C, corresponded to an imine reaction of the amide group and the thermal decomposition of hydrophobic side chains.[4,43,44] Stage 2 occurred beyond 350°C. At about 450°C, all of poly(acrylamide-co-N-hexadecyla-crylamide)s [poly(Am-co-hAm)s] and PAM were decomposed completely, and the thermogravimetric curves were flattened and no longer changed. This part of the weight loss may have been due to the thermal decomposition of the copolymer backbone. The results show the good thermal stability of the copolymers. However, different modes of alkyl distribution in P_1 and P_3 affected the first stage of decomposition. As shown, P_3, like PAM, exhibited two distinct weight losses between 200 and 250°C. Although P_1 exhibited one clear weight loss, which appeared in a lower temperature range (190–210°C), the second stages for P_1, P_3, and PAM occurred at 390, 400, and 400°C, respectively. The final residual weight of P_3 was higher compared to that of P_1; this implied that P_3 had better thermal stability.

Therefore, a homogeneous alkyl distribution gave rise to a more thermally stable copolymer at high temperature. TGA showed
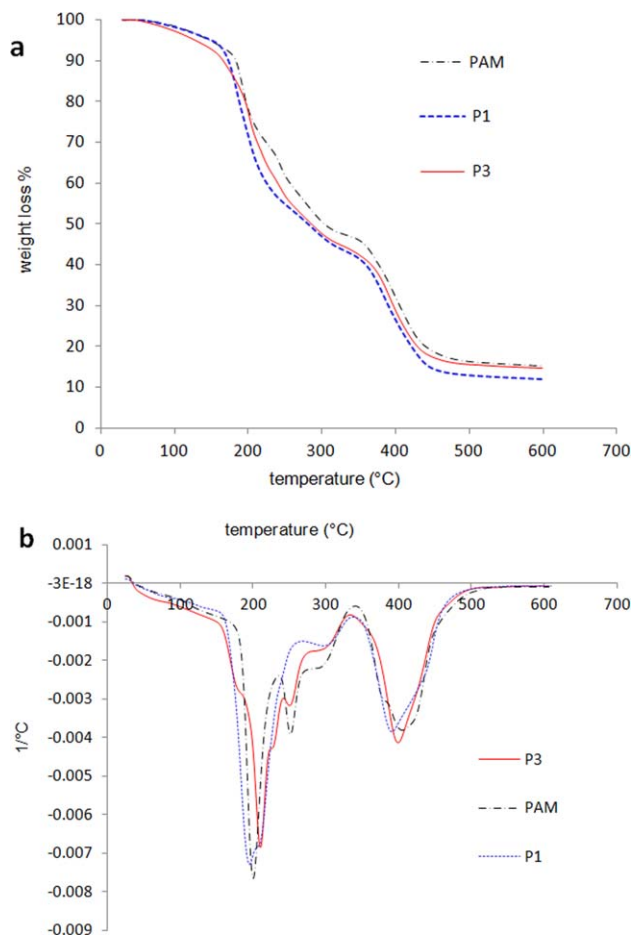

Figure 14. Thermograms of the polymers under an N_2 atmosphere at a heating rate of 20°C/min: (a) TGA and (b) DTGA. [Color figure can be viewed in the online issue, which is available at wileyonlinelibrary.com.]
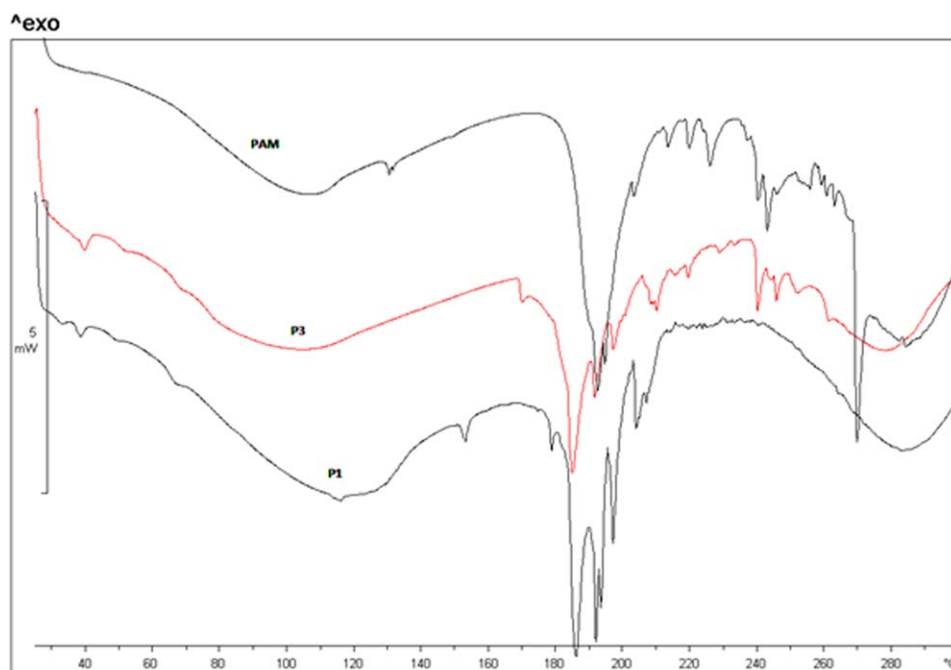

Figure 15. DSC diagrams of the polymers at a 20°C/min heating rate under an N_2 atmosphere. [Color figure can be viewed in the online issue, which is available at wileyonlinelibrary.com.]
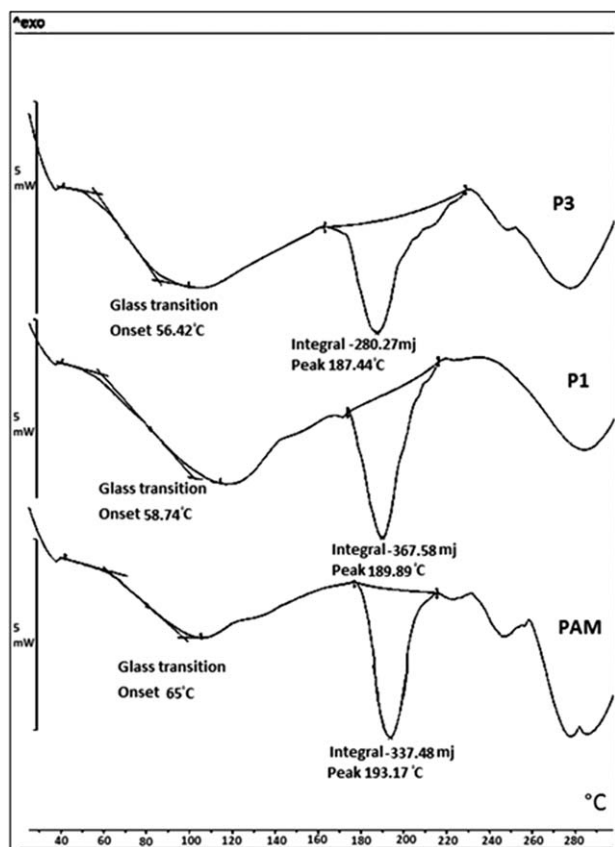
Figure 16. Smoothed DSC diagrams of the polymers at a heating rate of 20°C/min under an N_2 atmosphere.

that for the copolymer with homogeneous alkyl distribution, the final thermal stability was the same as that of PAM because of the uniform structure of both PAM and P_3.

DSC Analysis. The chain structure of the polymers was successfully characterized by DSC. Figure 15 shows a combination of the DSC curves of P_1, P_3, and PAM, and Figure 16 shows the areas under the melting peaks (melting enthalpy) and onset/midpoint T_g values of the polymers after the graphs were smoothed. The DSC curves of the copolymers were different from that of PAM. For PAM in the T_g area, one smooth transition appeared but for the copolymers; this transition had two small valleys. This different behavior in the T_g area was an indication of hAm inclusion in the copolymer backbone. A compar-
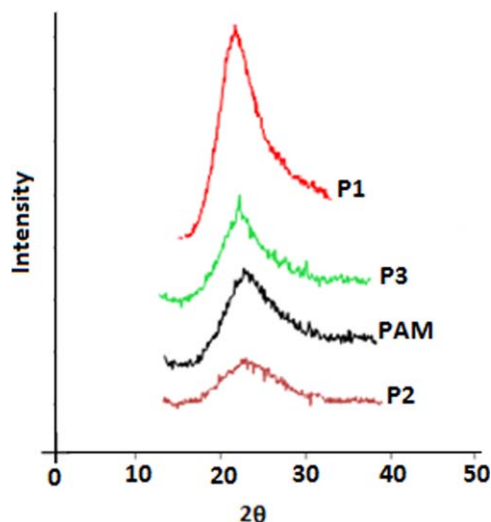

Figure 17. WAXD spectra of the copolymers and PAM at $2\theta = 10$–$40°$. [Color figure can be viewed in the online issue, which is available at wileyonlinelibrary.com.]

ison of the DSC curves of the copolymers with PAM showed a T_m peak of PAM with a quite uniform microstructure at 193°C, but for the copolymers, two branched peaks emerged in the T_m region, one sharp peak at 186°C and another peak at 193°C of the PAM T_m. So, with the inclusion of hAm in the PAM backbone, the T_m peak shifted to the lower temperature of 186°C. The peak at 193°C was very small for P_3, but this peak was sharp for P_1. Nonetheless, for P_3, in the presence of a surfactant (DBSA) in the reaction medium, the alkyl group distribution was more uniform, but for P_1, this distribution was in bulk with two sharp T_m's. Smoothed DSC curves showed the melting enthalpy (Joules per gram) of the copolymers; this also confirmed this result. The melting enthalpy of P_1 was higher than those of P_3 and PAM (Table IV). The homogeneous distribution of alkyl chains among the PAM domains in P_3 gave a space that prevented the amide groups from mutually interacting throughout the polymer backbone and so produced weaker hydrogen bonding, lower crystallinity, and lower melting enthalpy compared to PAM itself. P_1, with associative or blocky distribution, had a maximum T_m enthalpy. In such distribution, amide groups were closer together and formed stronger and tighter hydrogen bonding and so gave rise to additional crystallinity. The aggregation of alkyl groups in blocky sites through

Table IV. Thermal Properties Data of the Polymeric Samples Prepared via Different Methods

Polymer	Reaction media	Step 1	Step 2	Char yield (%)[a]	T_m[b]	T_g[c]	$\Delta T = T_{g, onset}$[d] $- T_{g, midpoint}$[e] (°C)	Melting enthalpy (J/g)
PAM	DMSO	200–250	400	15.04	193	65	15.5	65
P_1	DMSO	190–210	390	11.92	186	59	22.8	68
P_3	DMSO + DBSA	210–253	400	14.77	186	56	14.3	56

[a] The percentage of the weight residue of the polymer sample at 600°C in an N_2 atmosphere by TGA.
[b] T_m of the copolymers recorded by DSC in an N_2 atmosphere.
[c] T_g of the polymer recorded by DSC in an N_2 atmosphere and determined at the onset of the stage.
[d] T_g was recorded at the onsetpoint of the transition in the heat capacity taken from DSC results.
[e] T_g was recorded at the midpoint of the transition in the heat capacity taken from DSC results.
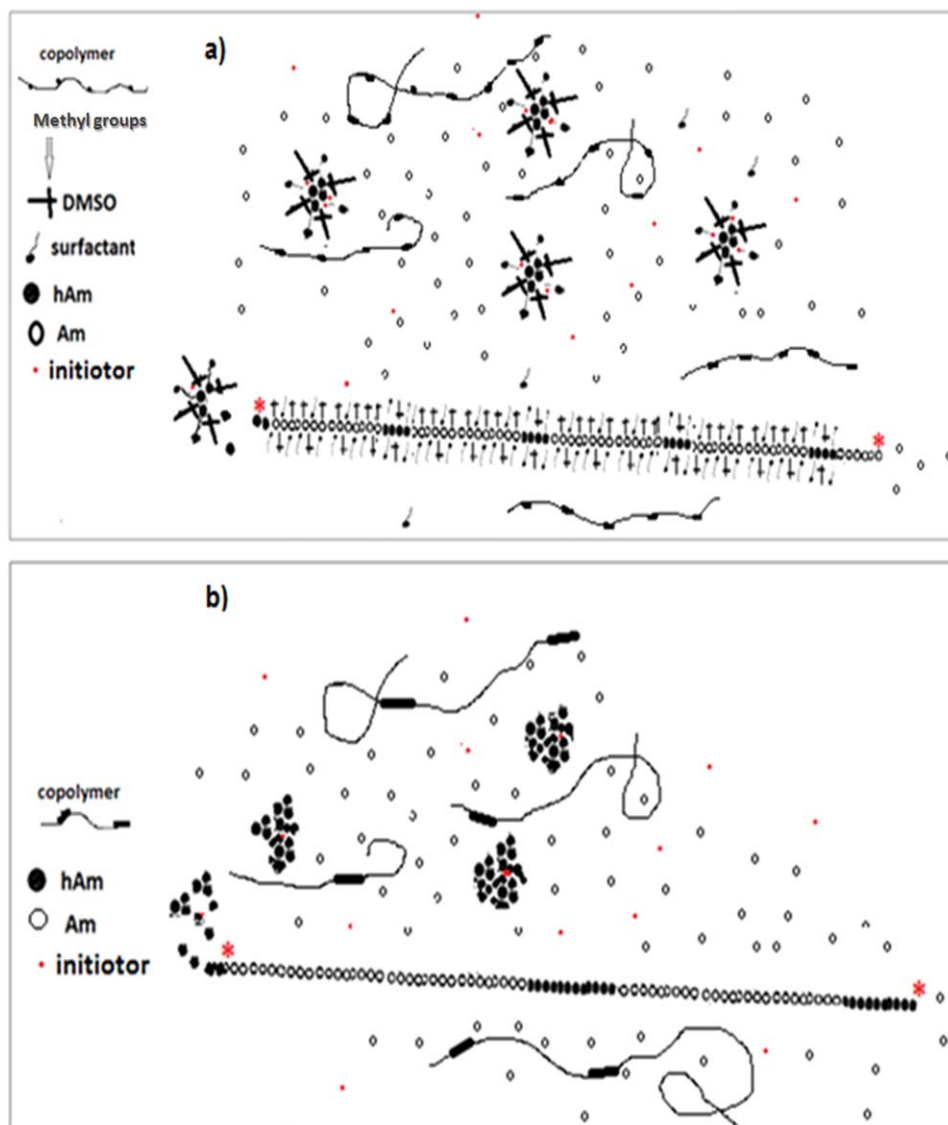
Figure 18. Schematic representations of different reaction media for poly(Am-*co*-hAm) in DMSO in the (a) presence and (b) absence of surfactant. [Color figure can be viewed in the online issue, which is available at wileyonlinelibrary.com.]

intermolecular interactions enhanced crystal formation in a blocky distribution. The distance between the onset and midpoint of T_g also demonstrated the mode of hydrophobic chain distribution, as presented in Table IV. For P_3, this ΔT ($[T_{g, \text{onset}} - T_{g, \text{midpoint}}]$) was close to that of PAM, and it was lower than P_1; this may have confirmed its homogeneous backbone compared to the blocky distribution of hydrophobic chains in P_1. With the inclusion of hAm in the PAM backbone, T_g was reduced ($T_{g,\text{PAM}} = 65°C$, $T_{g,P3} = 56°C$, $T_{g,P1} = 59°C$). Weaker interchain interactions, due to steric hindrance created by the hexadecyl group in hAm, resulted in a lower T_g. The results based on the T_g values of polymers also confirmed the correct prediction on the mode of distribution made in the polymer backbone. In case of P_3, there was better chain mobility because of better alkyl group distribution, which produced a lower T_g. Because of the associative entanglement of hexadecyl chains in P_1, there were more hindered chains, a lower mobility, and a

higher T_g compared to P_3. The T_g peak in P_3 was broad compared to that of P_1. This was because of a more homogeneous hAm distribution in the P_3 backbone. Moreover, as shown in Figure 15, there were some fluctuations in the thermogram of PAM above 220°C. In our opinion, these fluctuations were presumably caused by the evaporation of the solvent and moisture absorbed by Am units in PAM, which resulted in maintenance of these two molecules in the samples until high temperatures even when degradation reactions occurred. However, in the presence of a hydrophobe, the absorption of solvent molecules decreased (see the thermograms of P_1 and P_3 in Figures 15 and 16).

X-Ray Diffraction (XRD) Patterns of the Polymers
Figure 17 shows the XRD results of the copolymers and PAM. Pure PAM showed a typical noncrystalline pattern, and the copolymers also totally showed the same pattern as PAM

because of the low number of alkyl chain groups in copolymer backbone. Nevertheless, the maximum points for the peaks of all of the copolymers shifted to higher 2θ values. Although the PAM $2\theta = 20.57$, there were shifts to $2\theta = 21.29$ for P_1, $2\theta = 21.77$ for P_2, and $2\theta = 21.41$ for P_3. This showed that the noncrystalline nature of PAM was retained in the copolymers, but because of the addition of an alkyl chain of the comonomer, the position of the crystal layer was changed, and the domain in the angle of diffraction (θ) was different. In the range of XRD pattern for alkyl chain ($2\theta = 12$–$27°$) [45] the XRD profile was narrow, and sharper domains appeared for P_1, P_2, and P_3 compared to PAM due to presence of alkyl groups in the copolymers. The XRD patterns of P_2 and P_3 were the same, and they were a little different from P_1 because of the different crystal layer positions in the copolymer synthesized in the presence of the surfactant.

Model of the Reaction Media

According to the data obtained from copolymer analysis, a model for the reaction media was developed that shows how the hydrophobic monomer was distributed in the polymer backbone.

A random and homogeneous distribution of the hydrophobic monomer in the polymer backbone was developed for the copolymer synthesized in the presence of a surfactant. On the basis of our proposed model, shown in Figure 18(a), the first hydrophobic monomer (hAm) molecules were distributed within several surfactant micelles, and then, Am was dissolved in continuous medium, and the KPS, which was dissolved in the same medium and in the micelles, initiated the polymerization of Am in the continuous medium. When the radical ends of the growing macroradical encountered monomer swollen micelles, they joined with the hAm chain molecules inside the micelle and formed short hydrophobic blocks. As shown in Figure 18(b), this process was repeated until a homogeneous microstructure of the copolymer was obtained.

For copolymer in the absence of a surfactant, the model demonstrates that the hydrophobic monomer molecules formed hydrophobic drops in the solvent medium because of the high-surface-tension intermolecular forces. In these drops, the initiator molecules could not diffuse well, and low-active hAm molecules reacted together by low KPS inside the drops. The reaction of these hydrophobic semiheterogeneous droplets with the PAM macroradicals resulted in a blocky microstructure for the copolymer [Figure 18(b)].

CONCLUSIONS

Three copolyacrylamides based on hAm were successfully synthesized by the reaction of Am with hAm in different reaction media. Polymerization was performed in DMSO as a solvent and in the presence of two surfactants, SDS and DBSA. Some experimental results were compared with PAM as a reference. The copolymers showed good thermal stability and good rheological behavior. The copolymers that were prepared in the presence of a surfactant displayed good rheological behavior with thickening properties, and the copolymer that was pre-

pared in the presence of DBSA maintained this thickening at a wider shear rate range.

Thermal studies showed that the copolymers displayed good thermal stability, and those prepared in the presence of a surfactant showed higher thermal stability compared to the copolymers prepared in the absence of a surfactant.

We believe that the different properties of the copolymers were due to the distributions of the hydrophobic groups in the chains. This study was designed to show a new synthetic route with superior properties to overcome the problems of mixing oil-soluble and water-soluble monomers in a one-component solvent as a microhomogeneous medium and to show the ability of microhomogeneous reaction media to efficiently copolymerize through high monomer reactivity for a shorter time. Moreover, with addition of the surfactant in DMSO, a homogeneous distribution of hydrophobic monomer was obtained in this new medium.

REFERENCES

1. Rico-Valverde, J. C.; Jiménez-Regalado, E. *J. Polym. Bull.* **2009**, *62*, 57.

2. Karloson, L.; Thuresson, K.; Lindman, B. *Carbohydr. Polym.* **2002**, *50*, 219.

3. Zhu, Z.; Jian, O.; Paillet, S.; Desbriéres, J.; Grassl, B. *Eur. Polym. J.* **2007**, *43*, 824.

4. Yang, Z. L.; Gao, B. Y.; Li, C. X.; Yue, Q. Y.; Liu, B. *Chem. Eng. J.* **2010**, *161*, 27.

5. Ren, H.; Li, Y.; Zhang, S.; Wang, J.; Luan, Z. *Colloid Surf. A* **2008**, *317*, 388.

6. Lin, Y.; Kaifu, L.; Ronghua, H. *Eur. Polym. J.* **2000**, *36*, 1711.

7. Penott-Chang, E. K.; Gouveia, L.; Fernández, I. J.; Müller, A. J.; Díaz-Barrios, A.; Sáez, A. E. *Colloid Surf. A* **2007**, *295*, 99.

8. McCormick, C. L.; Lowe, A. B.; Ayres, N. In Kirk–Othmer Encyclopedia of Chemical Technology; Wiley: Hoboken, NJ, **2006**.

9. Xue, W.; Hamley, I. W.; Castelletto, V.; Olmsted, P. D. *Eur. Polym. J.* **2004**, *40*, 47.

10. Hussein, I. A.; Mozumder, M. S.; Abu Sharkh, B. F.; Ali, S. A.; Al-Naizy, R. *Eur. Polym. J.* **2005**, *41*, 2472.

11. Wever, D. A. Z.; Picchioni, F.; Broekhuis, A. A. *Prog. Polym. Sci.* **2011**, *36*, 1558.

12. Abidin, A. Z.; Puspasari, T.; Nugroho, W. A. *Proced. Chem.* **2012**, *4*, 11.

13. Taylor, K. C.; Nasr-El-Din, H. A. *J. Pet. Sci. Eng.* **1998**, *19*, 265.

14. Yao, L.; Chen, P.; Ding, B.; Luo, J.; Jiang, B.; Zhou, G. *J. Mol. Model.* **2012**, *18*, 4529.

15. Gong, L. X.; Zhang, X. F. *Express. Polym. Let.* **2009**, *3*, 778.

16. Zhang, X. F.; Wu, W. H. *Chin. Chem. Let.* **2009**, *20*, 1361.

17. Hill, A.; Candau, F.; Selb, J. *Macromolecules* **1993**, *26*, 4521.

18. Zhong, C.; Luo, T.; Deng, J. *Polym. Bull.* **2009**, *63*, 709.

19. Xiaowu, Y.; Yiding, S.; Peizhi, L. *Polym. Bull.* **2010**, *65*, 111.

20. Zhong, C.; Huang, R.; Xu, J. *J. Solution Chem.* **2008**, *37*, 1227.

21. Feng, Y.; Billon.; L., Grassl, B.; Khoukh, A.; Francois, J. *Polymer* **2002**, *43*, 2055.

22. Miller-Chou, B. A.; Koenig, J. L. *Prog. Polym. Sci.* **2003**, *28*, 1223.

23. Deguchi, S.; Lindman, B. *Polymer* **1999**, *40*, 7163.

24. Vignes, R. Presented at the ACS Annual Meeting, Washington, DC, August **2000**.

25. Chakrabarti, R.; Schutt, C. E. Gene. **2001**, *274*, 293.

26. Gupta, S. N.; Nandi, U. S. *J. Polym. Sci. Part A: Polym. Chem.* **1970**, *8*, 1493.

27. Kurenkov, V. F.; Antonovich, O. A. *Russ. J. Appl. Chem.* **2003**, *76*, 280.

28. Thomas, D. B.; Convertine, A. J.; Myrick, L. J.; Scales, C. W.; Smith, A. E.; Lowe, A. B.; Vasilieva, Y. A.; Ayres, N.; McCormick, C. L. *Macromolecules* **2004**, *37*, 8941.

29. Lele, B. S.; Gore, M. A.; Kulkarni, M. G. *J. Appl. Polym. Sci.* **1999**, *73*, 1845.

30. Johans, C.; Suomalainen, P. "Delta-8 multichannel microtensiometer: Influence of DMSO on the CMC of SDS". http://www.kibron.com, **2004**.

31. Holmberg, K.; Jonsson, B.; Kronberg, B.; Lindman, B. Surfactants and Polymers in Aqueous Solution; Wiley: Hoboken, NJ, **2003**.

32. Volpert, E.; Selb, J.; Candau, F. *Polymer* **1998**, *39*, 1025.

33. Candau, F.; Selb, J. *Adv. Colloid Interface Sci.* **1999**, *79*, 149.

34. Yahaya, G. O.; Ahdab, A. A.; Ali, S. A.; Abu-Sharkh, B. F.; Hamad, E. Z. *Polymer* **2001**, *42*, 3363.

35. Peer, W. *J. Polym. Mater. Sci. Eng.* **1987**, *57*, 492.

36. Maerker, J. M.; Sinton, S. W. *J. Rheol.* **1986**, *30*, 77.

37. Jenkins, R. D.; Silebi, C. A.; El-Asser, M. S. *ACS Symp. Ser.* **1991**, *462*, 222.

38. Yahya, G. O.; Asrof Ali, S. K.; Al-Naafa, M. A.; Hamad, E. Z. *J. Appl. Polym. Sci.* **1995**, *57*, 343.

39. Yahya, G. O.; Hamad, E. Z. *Polymer* **1995**, *36*, 3705.

40. Kopperud, H. M.; Hansen, F. K.; Nystrom, B. *Macromol. Chem. Phys.* **1998**, *199*, 2385.

41. Shaikh, S.; Asrof Ali, S. K.; Hamad, E. Z.; Abu-Sharkh, B. F. *Polym. Eng. Sci.* **1999**, *39*, 1962.

42. McCormick, C. L.; Nonaka, T.; Johnson, C. *Polymer* **1988**, *29*, 731.

43. Thakur, A.; Wanchoo, R. K.; Singh, P. *Chem. Biochem. Eng. Q.* **2011**, *25*, 471.

44. Lee, K. E.; Khan, I.; Morad, N.; Teng, T. T.; Teik Poh, B. Society of Plastics Engineer Plastics Research Online [Online] **2011**. DOI: 10.2417/spepro.003873. http://www.4spepro.org/view.php?source=003873-2011-10-14.

45. Milhet, M.; Pauly, J.; Coutinho, J. A. P.; Dirand, M.; Daridon, J. L. *Fluid. Phase Equilib.* **2005**, *235*, 173.